Effective Reinforcement of Carbon Nanotubes in Polypropylene Matrices

H. Deng,[1,2] E. Bilotti,[1,2] R. Zhang,[1,2] T. Peijs[1,2,3]

[1]*Centre for Materials Research, Queen Mary University of London, London E1 4NS, United Kingdom*
[2]*School of Engineering and Materials Science, Queen Mary University of London, London E1 4NS, United Kingdom*
[3]*Eindhoven University of Technology, Eindhoven Polymer Laboratories, Eindhoven 5600 MB, The Netherlands*

Received 20 December 2009; accepted 16 May 2009
DOI 10.1002/app.30783
Published online 13 May 2010 in Wiley InterScience (www.interscience.wiley.com).

ABSTRACT: This study describes an attempt to mechanically reinforce polypropylene (PP) using multi-wall carbon nanotubes (MWNTs) through a melt compounding process followed by hot-pressing and solid state drawing. The effect of a high density polyethylene (HDPE) coating on MWNTs and melt flow index (MFI) of PP on the dispersion of MWNTs and composite properties are studied by means of mechanical tests, transmission electron microscopy (TEM), scanning electron microscope (SEM), differential scanning calorimetry (DSC), and wide angle x-ray diffraction (WAXD). Highly orientated composite tapes are prepared to fully utilize the properties of MWNTs in uniaxial direction. Highly aligned MWNTs are shown by SEM, while highly oriented polymer chains are characterized by WAXD. Composite theory is used to analysis the results and indicates that effective reinforcement of PP by MWNTs is highest at relatively low filler content and draw ratios. © 2010 Wiley Periodicals, Inc. J Appl Polym Sci 118: 30–41, 2010

Key words: nanocomposites; carbon nanotubes; polypropylene; fibres; mechanical properties

INTRODUCTION

Carbon nanotube (CNT) polymer composites have been extensively investigated since CNTs have a combination of superior mechanical, electrical and thermal properties, which makes them one of the most attractive fillers for polymers.[1–7] Many investigations have been published with a range of improvements in different properties.[7–13] The first proof of concept of nanotube-polymer composites was published by Ajayan et al.[11] Since then, a large number of papers have been published in this area, including a number of review articles focused on various aspects of polymer/CNT composites,[1–7] however, so far only a limited studies have shown effective reinforcement of polymer by CNTs.[7,12]

Given the importance of polypropylene (PP) as an engineering polymer, surprisingly few papers have been published on PP based composites incorporating nanotubes.[13–24] Both solvent processes and melt compounding processes have been used to create these composites. In one of the first studies on PP/CNT composites, Andrews et al.[13] fabricated PP/MWNT composites in a shear mixer. A modulus increase was found from 1.0 GPa to 2.4 GPa at a fairly high MWNT content of 12.5 wt %. However, the yield strength decreased from 30 MPa to 18 MPa, with the yield strain also decreasing with increasing MWNT content. A number of other studies have been carried out on PP/CNT composites, but only a few of them have reported mechanical properties of bulk composites. The data obtained by Manchado et al.[19] is one of the best among all; they fabricated PP/SWNT composites by melt blending. The modulus increased from 0.85 GPa to 1.19 GPa at a fairly low nanotube loading of 0.75 wt %, while the tensile strength increased from 31 MPa to 36 MPa for systems incorporating 0.5 wt % SWNTs. However, both these properties, including strain at break decreased at higher nanotube loadings. Ganb et al.[24] also carried out investigations on PP/CNT composites, but their reported increase in mechanical properties was not significant. Their DMA study showed also a lowering of the glass transition temperature (T_g) after the addition of MWNTs.

Overall, it can be concluded that the reported mechanical reinforcement of CNTs in isotropic PP matrices is moderate, with the most efficient reinforcement observed at very low nanotube loadings, possibly due to poor dispersion of the CNTs at higher loadings.

High-performance polymer fibres or tapes have become active area of research since the 1930s.[25,26] Research activities on this topic have led to a range of successful commercial products: such as Dyneema® [27] and Kevlar®.[28] Under the pressure of

Correspondence to: T. Peijs (t.peijs@qmul.ac.uk).

environmental and recycling issues, recent development in orientated polymers has concentrated on self reinforced polymer composites. Achievements from Ward and Hine[29] and Peijs and co-workers[30–45] were developed into commercialised products under the trade names of Curv® and PURE®, respectively. Because of the one-dimensional (1D) structure of CNTs, oriented polymer/CNT composite fibres or tapes attracted much attention as the incorporation of 1D nanofillers in 1D objects like fibres or tapes result in a high mechanical reinforcing efficiency.[7,12] In the following section, the mechanical reinforcement of CNTs in highly oriented PP fibres or tapes is reviewed.

Solvent mixing and melting spinning was used to produce PP/SWNT fibres by Kearns et al.[46] The spun fibre was post-drawn which lead to excellent mechanical properties. They obtained a modulus increase from 6.3 GPa to 9.8 GPa with 1 wt % of SWNTs. The strength increased from 709 MPa to 1027 MPa at 1 wt % for a draw ratio of eight. Furthermore, the elongation at break increased from 19% to 27%, which means an increase in toughness with the addition of SWNTs. Two years later, the same group fabricated PP/SWNT fibres from two different grades of PP: high and low melt-flow index (MFI) polymer.[47] The modulus was observed to increase only for low MFI PP, due to the better dispersion of the SWNTs in the higher molecular weight polymer, indicating the importance of selecting the right polymer grade for CNT based nanocomposites. It is worth mentioning that higher loadings (>1 wt %) resulted in lower moduli and strengths than lower loadings (<1 wt %).

Soon after, Bhattacharyya et al. produced PP/SWNT fibres using a simple melt spinning method.[15] X-ray diffraction (XRD) and polarized Raman spectroscopy were used to study the orientation of SWNTs in the fibre. However, mechanical properties including strength, modulus and elongation at break decreased with the addition of SWNTs. Again, poor dispersion of the SWNTs in the PP matrix was responsible for this. Chang et al.[16] fabricated PP/SWNT composites by a solvent casting method, which was then melt spun into a fibre. A modulus increase from 0.4 GPa to 1 GPa at 1 wt % SWNTs was observed. The modulus remained at the same value for systems with 2 wt % to 5 wt % SWNTs. The elongation at break of all loadings was not shown in this study, which might indicate embrittlement due to poor dispersion at higher loadings. However, tensile strength did increase from 4 MPa to 20 MPa at 5 wt % SWNTs, and significant stress transfer between polymer matrix and SWNTs was observed by Raman spectroscopy.

Dondero et al. fabricated PP/MWNT fibres by a simple melt mixing and melt drawing method.[48] Microscopy studies showed poor dispersion of MWNTs in PP. Despite this the drawn fibres showed a significant increase in Young's modulus from 611 MPa to 1250 MPa at only 0.25 wt % MWNTs. However, further addition of MWNTs showed a reduction in modulus. In addition, differential scanning calorimetry (DSC) studies revealed little change in overall crystallinity with the presence of MWNTs. Finally, Jose et al.[49] reported a study on melt spun PP/MWNT fibres. The modulus of these fibres increased from 1.67 GPa to 3.5 GPa with 1 wt % of MWNTs, while the strength increased from 330 MPa to 420 MPa. Good dispersion and orientation of the MWNTs was observed in the polymer fibre by TEM. However, the draw ratio they achieved was relatively low, hence leading to fairly low overall mechanical properties.

Until now, several studies on oriented PP/CNT fibres have been reviewed. Some studies[46,49] show good mechanical reinforcement by CNTs, some of them do not.[47,48] It should also be noted that most studies found that large amounts of CNTs in polymer fibres or tapes (>1 wt %) do not increase the mechanical properties as effectively as low CNT contents (<1 wt %).

A further comment needs to be made on the effect of the molecular weight of the PP, which seems to play an important role in the dispersion of nanofillers,[50] and will be discussed in this study. Good dispersion, good interfacial interaction and high orientation of the CNTs are considered to be crucial for effective mechanical reinforcement in CNT/polymer composites.[12] Current study will address these issues by using HDPE coated MWNTs and drawing composites to high draw ratio, in order to fully align the nanotubes. Finally, micromechanical modeling is used to analyze the true mechanical reinforcing efficiency of MWNTs in PP.

EXPERIMENTAL

Materials and composites preparation

The polypropylene used in this project is Moplen HP500H (MFI = 1.8 g/10 min), Moplen 400R (MFI = 25 g/10 min) and Dow H507 (MFI = 3.2 g/10 min), kindly supplied by Basell and DOW, respectively. They are referred to as PP 1.8, PP 3.2, and PP 25 in this study. The HDPE coated MWNT (cMWNTs) as described in[3] with a nanotube content of 31.6 wt % (NC9000) and industrial grade MWNT (NC7000) were kindly supplied by Nanocyl S.A. (Belgium). MWNTs were blended with the three polymer grades in a mini-extruder (DSM Micro 15) at 200°C. First, a masterbatch containing 3 wt % NC9000 (or NC7000) was made at the processing condition of 50 rpm for 5 min before being diluted

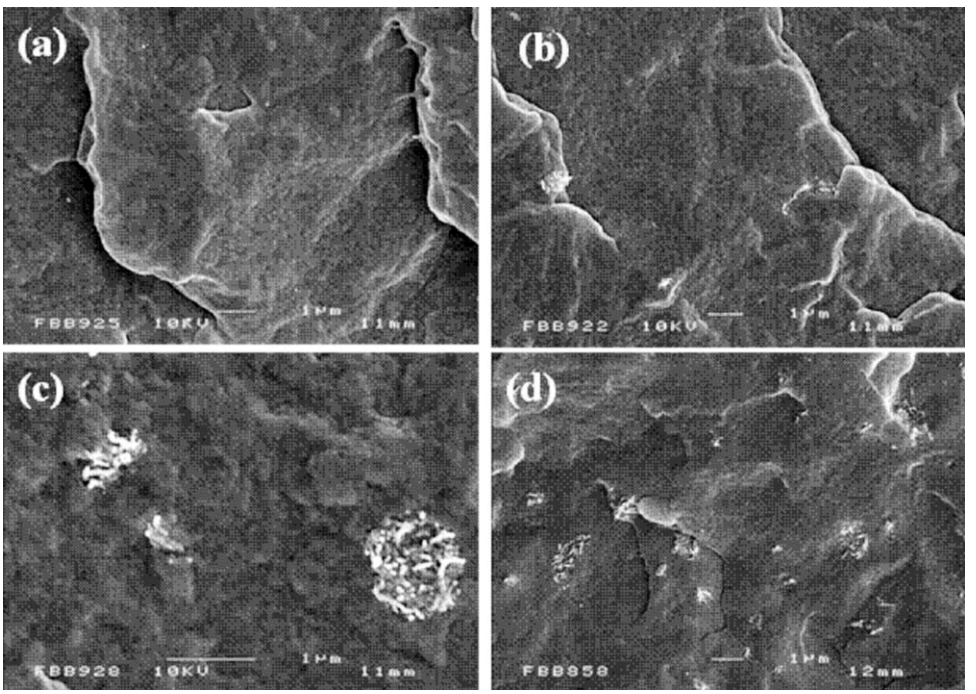

Figure 1 SEM pictures of (a) 0.1 wt % coated MWNTs in PP 1.8, (b) 0.1 wt % coated MWNTs in PP 3.2, (c) 0.1 wt % coated MWNTs in PP 25, (d) represents 1 wt % MWNTs and MWNTs in all PP 1.8, 3.2, and 25 as no difference in dispersion is observed for these specimens under SEM.

into the required nanotube concentrations at 250 rpm for 15 min. Nitrogen gas flow was used to avoid degradation of the polymer during the mixing process. All the neat PPs investigated in this study have been through the same extrusion process as the composites to give them the same thermal history. The strands exiting the extruder were cut into pellets and then hot pressed into dumbbell shaped tensile specimen according to ASTM 638 at 200°C under 40 MPa for 5 min. The samples were cooled down to room temperature using the water cooling system of the hot press. Neat PP 3.2 pellets and PP 3.2 pellets containing cMWNTs or MWNTs were hot pressed into film with a thickness near 0.1 mm. The films

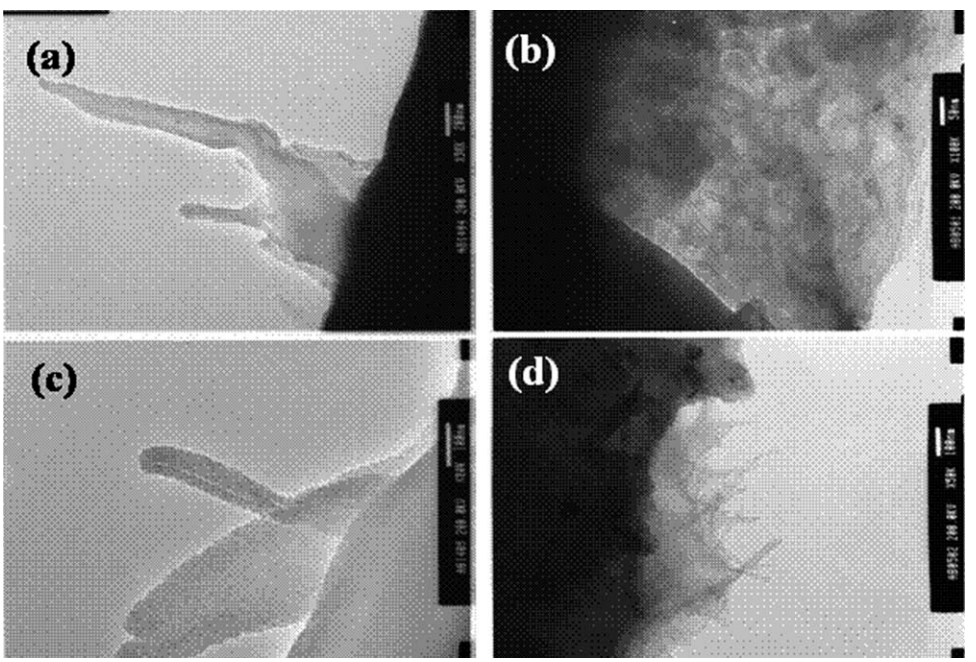

Figure 2 TEM pictures of (a, c) cMWNTs and (b, d) MWNTs in PP 1.8 matrix.

TABLE I
Melting Temperature Obtained From DSC (Second Melting Peak) of the Polymer and Composites Studied

cMWNT content	PP1.8 [° C]	STD [± ° C]	PP3.2 [° C]	STD [± ° C]	PP25 [° C]	STD [± ° C]
0 wt %	166.04	0.67	164.56	1.03	165.67	1.43
0.1 wt %	164.47	0.04	165.66	0.84	163.67	0.37
0.25 wt %	164.50	0.34	165.15	0.35	164.92	0.46
0.5 wt %	166.55	1.37	165.39	0.26	164.53	0.17
0.75 wt %	164.45	2.16	165.14	0.58	165.39	0.20
1 wt %	165.42	1.13	164.86	1.05	164.25	0.01
1 wt % MWNT	164.97	0.18	165.16	1.72	164.63	0.89

STD: standard deviation.

were cut into 5 mm × 40 mm strips and drawn in the solid state to highly oriented PP tapes.[50] The drawing was conducted in the environmental chamber of an Instron 5584 tensile test machine at 120°C at a cross-head speed of 50 mm/min.

Composites characterization

Morphological studies are carried out in a scanning electron microscope (SEM) (JEOL JSM-6300F), on gold-coated, cold fracture surfaces. SEM in contrast mode is also used to study the highly oriented tapes to reveal the CNT network within the composites. The morphology of cMWNTs and MWNTs in the polymer matrix is examined by transmission electron microscopy (TEM) (JEOL JEM-2010). Samples are prepared using a Gatan, Precision Ion Polishing System (PIPS)-691.

Tensile tests are performed on an Instron 5566 equipped with a video extensometer. The gauge length and cross-head speed used for bulk composite testing is 30 mm and 10 mm/min. The test condition used for the drawn tapes was 30 mm and 30 mm/min.

Differential scanning calorimetry (DSC) was performed under nitrogen gas flow in the range of 20–200°C, using a Mettler Toledo DSC 822^e. Samples were heated to 200°C and held there for 5 min to remove the previous thermal history after which they were cooled to 20°C. The DSC scanning rate was 10°C/min.

Dynamic mechanical thermal analysis (DMA) is performed on the isotropic composites using a TA Instruments Q800 machine equipped for tension mode. The temperature scans range from −30°C to 150°C at a rate of 3°C/min. A frequency of 1 Hz and strain of 0.3 % is chosen for the test. The sample are cut into 30 mm × 3 mm strips from hot pressed film (thickness: ∼ 100 μm), and the gauge length is set at 20 mm.

Two-dimensional wide angle X-ray diffraction (WAXD) patterns are recorded in transmission mode by a CCD camera with an exposure time of 60 s. The X-ray source is a synchrotron radiation, beam line BM26 Dubble (Dutch-Belgian beam line) at ESRF (European Synchrotron Radiation Facility). The average wavelength was 1.24 Å.

RESULTS AND DISCUSSION

Morphology of the composites

As described in the experimental section 0.1 to 1 wt % cMWNTs and 1 wt % MWNTs are melt compounded with PP 1.8, PP 3.2, and PP 25 in a mini-extruder, respectively. The morphology of 0.1 wt % cMWNTs in PP 1.8, PP 3.2, and PP 25 is shown in Figure 1(a–c), respectively. It is clear that the lower melt index PP gives the best CNT dispersion. The higher viscosity of the polymer is responsible for higher internal shear forces in the extruder, and more energy generated for dispersion.[50]

TABLE II
Crystallization Temperature Obtained from DSC of the Polymer and Composites Studied

cMWNT content	PP1.8 [° C]	STD [±° C]	PP3.2 [° C]	STD [±° C]	PP25 [°C]	STD [±° C]
0 wt %	105.28	0.38	116.62	0.85	108.16	1.31
0.1 wt %	117.53	0.27	116.97	0.26	119.48	0.89
0.25 wt %	117.87	0.29	117.57	0.34	119.29	0.43
0.5 wt %	116.71	0.40	116.93	0.40	118.91	0.45
0.75 wt %	118.24	0.78	117.32	0.66	119.67	0.54
1 wt %	117.78	0.36	117.98	0.21	119.45	0.20
1wt % MWNT	121.91	0.22	122.36	0.99	125.37	0.54

STD: standard deviation.

TABLE III
Crystallinity Obtained from DSC (Second Melting Peak) of the Polymer and Composites Studied

cMWNT content	PP18 [%]	STD [± %]	PP3.2 [%]	STD [± %]	PP25 [%]	STD [± %]
0 wt %	37.92	1.37	40.57	1.26	39.93	2.34
0.1 wt %	41.43	1.05	39.90	1.72	44.95	1.24
0.25 wt %	39.98	1.05	41.44	1.29	44.29	0.10
0.5 wt %	38.88	0.71	40.95	2.27	43.13	1.79
0.75 wt %	40.92	0.32	40.48	2.17	43.76	0.12
1 wt %	39.83	1.10	41.00	0.92	42.98	1.16
1 wt % MWNT	40.16	2.75	42.56	1.45	44.04	3.10

STD: standard deviation.

As concluded by Huang et al.,[51] the higher the CNT loading in the polymer matrix, the more energy is needed to disperse the CNTs to achieve the same state of dispersion. However, polymer degradation and tube length cutting is also likely to occur under these conditions. Therefore, the same processing conditions are chosen for composites containing different amounts of CNTs. As a result, composites containing the highest loading of MWNTs (1 wt %) showed the worst dispersion for all three PP grades [see Fig. 1(d)]. However, no difference in state of dispersion can be observed using SEM for the different matrices containing 1 wt.% of coated MWNTs.

Both the cMWNT/PP composites and MWNT/PP composites were studied by TEM in order to visualize the polymer coating onto the nanotubes. As shown in Figure 2(a,c), there is an indication of the existence of a polymer coating on the MWNTs even after melt processing [see Fig. 2(b,d)]. TEM of composites incorporating non-coated MWNTs did not show such an interphase [see Fig. 2(b,d)]. The HDPE interphase between carbon nanotubes and PP matrix can help to improve dispersion and through this the reinforcing efficiency. Previously, studies on cMWNTs have shown that a good dispersion of cMWNTs can be achieved in EVA even if this polymer is immiscible with HDPE.[3] Therefore, in spite of PP being immiscible with HDPE, coated MWNTs have been used in order to achieve better dispersion and wetting of the nanotubes by the PP matrix.

Thermal analysis of the composites

The melting temperature, crystallization temperature and crystallinity of the polymer and composites investigated in this study are listed in Tables I to III, respectively. The effect of nanofillers on the melting temperature of the composites is negligible as shown in Table I. It remains around 165°C after the addition of coated MWNTs or MWNTs into the PP matrix. This indicates that PP crystals remain at α phase, since β phase PP crystals melt at lower temperature.[15] This agrees well with previous studies, where only α phase crystals were obtained by adding CNTs into PP matrix.[16,18,51]

The crystallization temperature of the composites is largely affected by the presence of CNTs as shown in Table II. Because of the nucleation effect of CNTs,[14,17,23] the crystallization temperature of PP 1.8 and PP 25 is increased by adding cMWNTs or MWNTs. The effect of increasing crystallization temperature in composites based on PP 3.2 is not that obvious. This might be due to the existence of a nucleation agent in this PP grade. Interestingly, the nucleation effect for MWNTs is much stronger than for coated MWNTs. Again, this could be considered as an indication of HDPE present at the interphase between MWNTs and PP.

The crystallinity of PP/MWNT composites and neat PP is shown in Table III. The crystallinity of PP 1.8 and PP 25 is increased by adding cMWNTs or MWNTs into the polymer matrix, while it remains nearly the same for PP 3.2. Thus, care should be taken when later considering the mechanical reinforcement of cMWNT or MWNT in PP matrices, as these effects could be due to a modification of the matrix through increased crystallinity.[12]

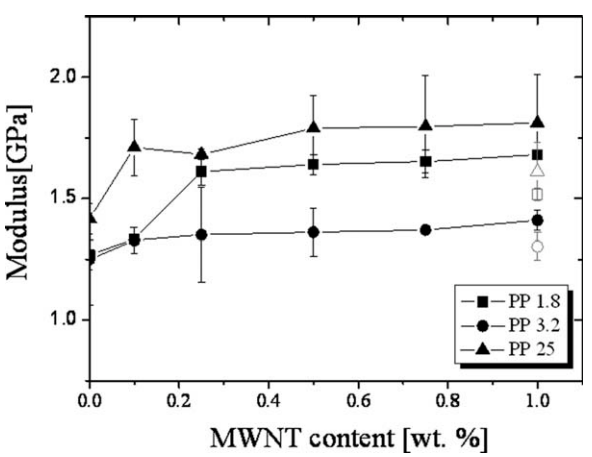

Figure 3 Young's modulus of bulk isotropic cMWNT/PP composites. Open symbols are for 1 wt % uncoated MWNTs.

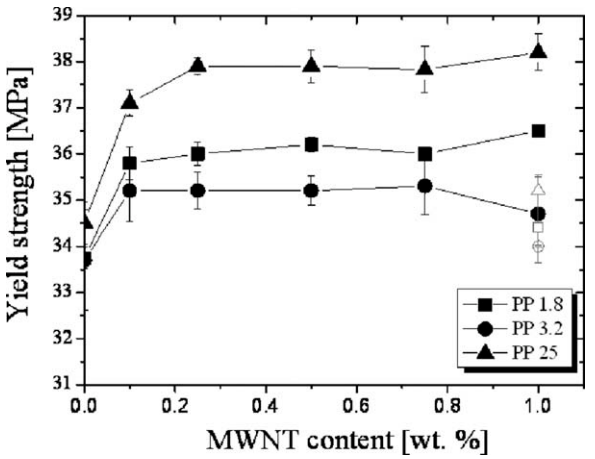

Figure 4 Yield strength of bulk cMWNT/PP composites. Open symbols are for 1 wt % uncoated MWNT composites.

Mechanical properties

Mechanical properties in terms of Young's modulus, yield strength and strain at break of the compression moulded PP/MWNT composites are shown in Figures 3–5, respectively. It was already shown in Figure 1 that the lower MFI polymers lead to a better CNT dispersion under similar processing condition. Figure 5 seems to confirm this by showing that composites based on PP 1.8 have the highest strain at break. According to polymer crystallization mechanisms,[52,53] composites based on PP 25 have a relative low strain at break as the cooling rate in the hot press is relatively slow, allowing polymer chains to grow into relative crystals. As a result there are less polymer chains connecting neighbouring crystals, leading to embrittlement. On the other hand, the low molecular weight PP grade leads to a higher crystallinity (see Table III) and thus higher modulus and yield stress as shown in Figures 3 and 4 for the composites based on PP 25.

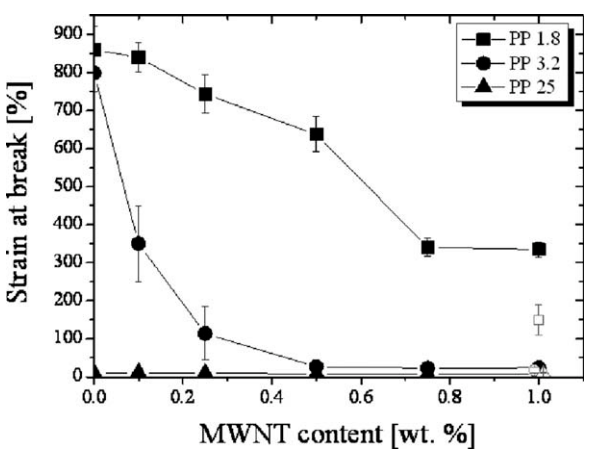

Figure 5 Strain at break of bulk cMWNT/PP composites, open symbols are results for 1 wt % uncoated PP/MWNTs.

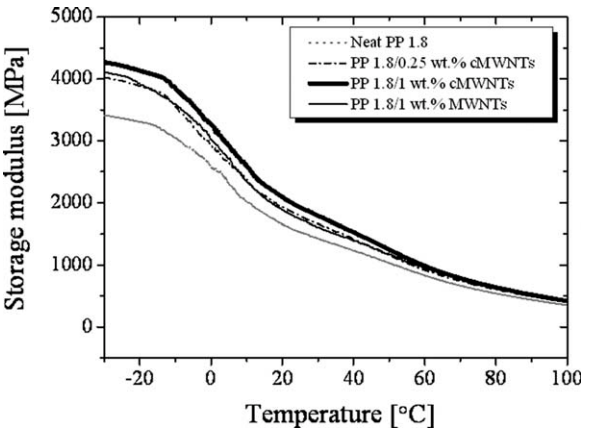

Figure 6 Storage modulus from DMA for cMWNT/PP composites based on PP 1.8.

It is interesting to note that again the highest properties are achieved at relatively low loadings (<0.5 wt %) of coated MWNTs which agrees with results reported in literature.[16,19] This again can be related to dispersion and is reflected by the decrease in strain at break with increasing coated MWNT content (see Fig. 5). Therefore, the optimum balance in terms of nanotube dispersion and mechanical properties seems to lie between 0.25 wt % and 0.5 wt %.

Furthermore, the better dispersion for cMWNT/PP (as shown in Fig. 2) is confirmed by comparing the mechanical properties of 1 wt % cMWNTs with those of 1 wt % MWNTs. It is clear that the HDPE coating leads to better dispersion and therefore better mechanical properties.

Figure 6 shows the results obtained from DMA tests for composites based on PP 1.8. The storage modulus (at 20°C) shows a similar increase in modulus as obtained for composites containing cMWNT or MWNT from tensile tests. Also here the composites with 1 wt % of HDPE coated MWNTs have a higher storage modulus than the composites containing the same amount of uncoated MWNTs. Similar results were obtained for composites based on PP 25. The storage modulus decreases with increasing temperature as shown in Figure 6, and the cMWNTs have improved the mechanical performance of the composites at elevated temperatures. For example, a storage modulus of 1.5 GPa is observed at 27°C for neat PP 1.8, while a similar modulus is obtained for 1 wt % cMWNT/PP composites at 41°C, showing the potential of MWNTs to improve the thermal stability of PP based composites.

It is believed that nanofillers in composites based on semi-crystalline polymers mainly exist in the amorphous phase.[24] However, transcrystalline layers around CNTs and reduced chain mobility near CNTs has also been observed.[54] The presence of nanofillers in the amorphous phase can change the

TABLE IV
Glass Transition Temperature Obtained from DMA for Composites Based on PP 1.8

cMWNT content	PP1.8 T_g (Loss modulus) [°C]	PP1.8 T_g (Tan δ) [°C]
0 wt %	4.12	9.06
0.25 wt %	3.62	9.10
1 wt %	1.82	7.62
1 wt % MWNT	1.73	7.91

TABLE V
Glass Transition Temperature Obtained from DMA for Composites Based on PP 25

cMWNT content	PP25 T_g (Loss modulus) [°C]	PP25 T_g (Tan δ) [°C]
0 wt %	2.48	8
0.25 wt %	0.89	6.64
1 wt %	0.38	5.67
1 wt % MWNT	−1.67	4.41

mobility of the polymer chains, which subsequently leads to changes in the glass transition temperature (T_g) of the polymer. Tables IV and V show the T_g (from DMA study) of the composites based on PP 1.8 and PP 25, respectively. T_g decreases with increasing CNT content for both matrices. A similar decrease in T_g with the addition of CNTs into a PP matrix has been reported previously.[24] In the current study, a similar decrease in T_g is obtained for both coated MWNT and MWNT based PP composites. The HDPE coating on the MWNTs does not seem to play a significant role on T_g for both PP 1.8 and PP 25 composites.

Orientated composite tapes

The composites based on PP 3.2 are drawn into tapes of different draw ratios to explore the potential of a uniaxial composite structure with both fully aligned polymer chains and carbon nanotubes. The morphology of these composites is studied as shown in Figure 7. Highly oriented coated MWNT bundles are observed in the solid-state drawn tapes, where the uniaxial orientation should significantly improve the stress transfer between the matrix and the nanotubes.[7,12]

The Young's modulus of the oriented tapes at different draw ratios is obtained from tensile tests as described previously. The general trend is that as expected the modulus increases with increasing draw ratio (Fig. 8).[55] However, the reinforcing effect of coated MWNTs in PP tapes is less pronounced in tapes of relative high draw ratio ($\lambda > 10$). This agrees well with previous studies, where relatively good reinforcement of CNTs or carbon nanofibres in PP fibres was obtained at relatively low draw ratios.[49,56] However, until now, no data was available on mechanical properties of PP/CNT fibres or tapes of high draw ratio ($\lambda > 15$).

The tensile strength of the tapes is shown in Figures 9 and 10. The strength increases with draw ratio for all composites until $\lambda \sim 20$, but further drawing of the tapes seems to decrease the tensile strength. The higher the draw ratio, the more organized the crystals are in the tape (see Fig. 11). Therefore, CNT bundles are more likely to act as crack initiators during deformation in highly oriented tapes. Another possible reason for this could be that further drawing above the minimum draw ratio needed to fully align the CNTs could destroy the interphase between the CNTs and the polymer matrix. CNTs and polymer chains are already highly oriented after drawing to ≈ 10 (see Figs. 7 and 11). In the case of well dispersed single-wall nanotubes in PVA it was reported by our group that CNTs are already highly aligned at draw ratios of around 5.[12] Hence, drawing above those draw ratios may lead to breakdown of the existing interphase (such as the HDPE coating) between polymer and nanotube. Similar effects may explain the observed trend for

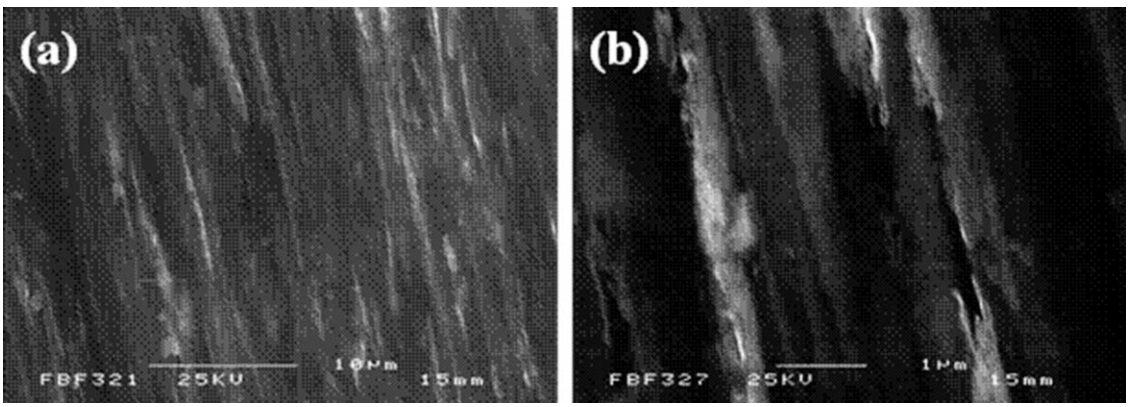

Figure 7 SEM picture showing highly oriented MWNTs bundles (1 wt % cMWNT/PP, $\lambda = 10$) at (a) low magnification, and (b) high magnification.

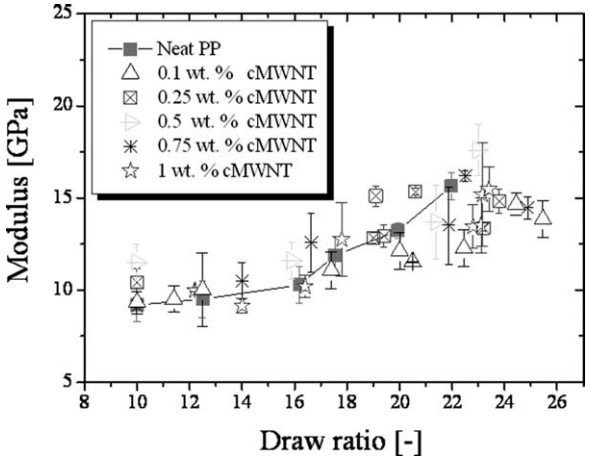

Figure 8 Young's modulus of orientated cMWNT/PP tapes at different draw ratios, showing a slight reduction in modulus of nanocomposite tapes compared to neat PP tapes.

modulus (Fig. 9). Finally, as expected the strain at break of the tapes decreases with increasing draw ratio with a small increase in strain at break for the nanocomposite tapes compared to the pure PP tapes (Fig. 10).

Wide angle X-ray diffraction (WAXD) is used to characterize the orientation of the polymer crystalline phase in the tapes at different draw ratios. Figure 11 shows the WAXD patterns of neat PP and 1 wt % coated MWNT/PP tapes at different draw ratios. The symmetric arcs indicate highly orientated PP crystals in the drawn tape. A sketch of a symmetric arc is shown in Figure 11(b), and indicates different positions of the peaks for α phase PP crystals in the pattern. Clearly, the alignment of the crystals is indicated by the reduced arc length upon drawing. Unfortunately, there is no clear signal for the coated MWNTs in the tapes by comparing the WAXD for neat PP tapes with those for 1 wt % coated MWNT/PP tapes.

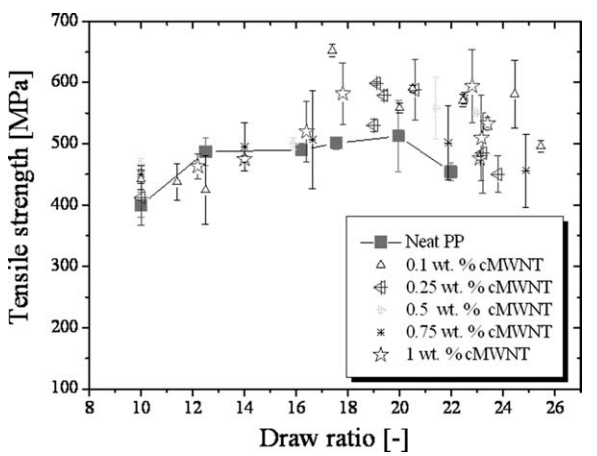

Figure 9 Tensile strength of orientated cMWNT/PP tapes at different draw ratios, showing a slight increase in tensile strength of nanocomposite tapes compared to neat PP tapes.

A quantitative measurement of polymer crystalline orientation could be obtained from Azimuthal scans of the diffraction rings, where the arcs are indicated as peaks.[12,57] The Azimuthal peaks are fitted with a Gaussian curve under the assumption that a uniaxial Gaussian distribution is obtained. From this, the well known Hermans' orientation factor[12,57,58] was calculated (Fig. 12). The crystal orientation function f_c is calculated from the Hermans' orientation equation, which can be expressed as follows:

$$f_c = \frac{3\langle \cos^2 \phi \rangle - 1}{2} \tag{1}$$

where $\langle \cos^2 \phi \rangle$ is obtained from following equation:

$$\langle \cos^2 \phi \rangle = \frac{\int_0^{\pi/2} I(\phi) \sin \phi \cos^2 \phi d\phi}{\int_0^{\pi/2} I(\phi) \sin \phi d\phi} \tag{2}$$

where ϕ is the Azimuthal angle. Perfect orientation in the drawing direction gives a value for $f_c = 1$, isotropic orientation gives a value for $f_c = 0$.

Hence, the PP crystals in both neat PP tapes and 1 wt % coated MWNT/PP tapes have similar degree of orientation as they have similar values for the Hermans' orientation factor at draw ratios of 5, 10, and 20, respectively (Fig. 12).

Composite micromechanics

Rule of mixtures

The rule of mixture can be used to calculate the effective reinforcement of fibres in composites systems. In the case of short fibre composites the modulus is given by [2,59]

$$E_c = \eta_L \eta_0 V_f E_f + (1 - V_f) E_m \tag{3}$$

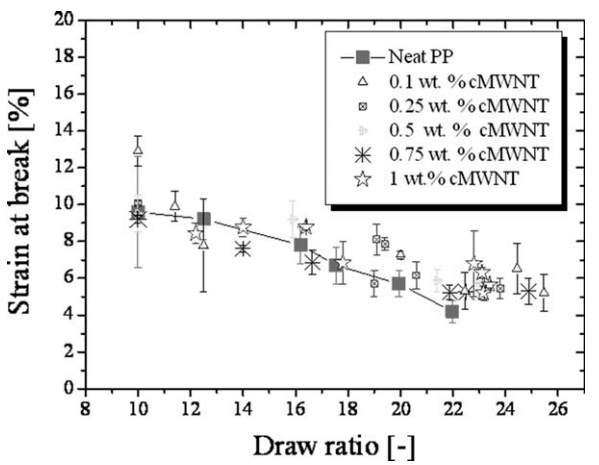

Figure 10 Strain at break of orientated cMWNT/PP tapes at different draw ratios, showing similar strain at break for nanocomposite tapes compared to neat PP tapes.

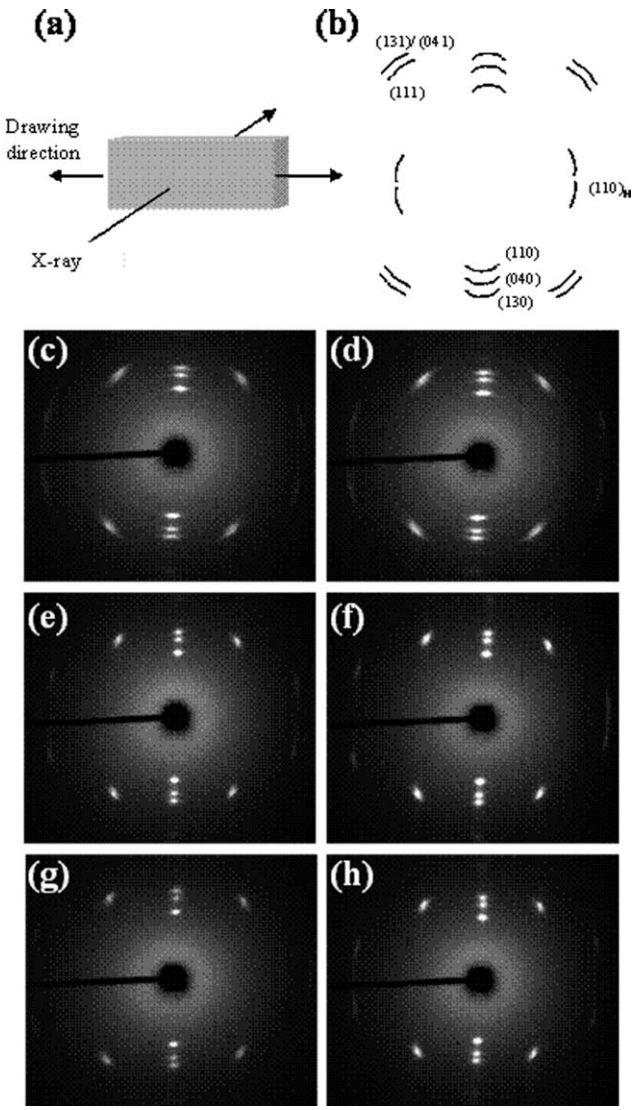

Figure 11 (a) Schematic set up for the Wide Angle X-ray Diffraction (WAXD) measurement; (b) schematic patterns of orientated PP; (c), (e) (g) WAXD patterns of neat PP tapes at $\lambda = 5$, 10, and 20, respectively; (d), (f), (h) WAXD patterns of cMWNT/PP tapes at $\lambda = 5$, 10, and 20, respectively.

Where η_0 is the orientation factor. This has the values of $\eta_0 = 1$ for fully aligned fibres (1D), $\eta_0 = 3/8$ for fibres aligned in-plane (2D) and $\eta_0 = 1/5$ for randomly oriented (3D) fibres.[2] η_L is the length efficiency factor, which approaches one for fibre aspect ratios (l/d) > 10, indicating that high aspect ratio fillers are preferred. E_c, E_f, E_m and V_f are the composites modulus, fibre modulus, matrix modulus and fibre volume fraction, respectively.

Similar calculation can be used to derive an equation for composite strength.[1]

$$\sigma_c = \eta_L \eta_0 V_f \sigma_f + (1 - V_f)\sigma_m \quad (4)$$

Therefore, eq. (3) and (4) can be used to evaluate the effective mechanical properties of CNTs in both isotropic and oriented composites. Figure 13 shows the back calculated effective modulus and tensile stress of cMWNTs in isotropic composites based on PP 3.2, assuming that $\eta_0 = 0.2$ and $\eta_L = 1$. Clearly, the effective properties of cMWNTs decrease with increasing filler content.

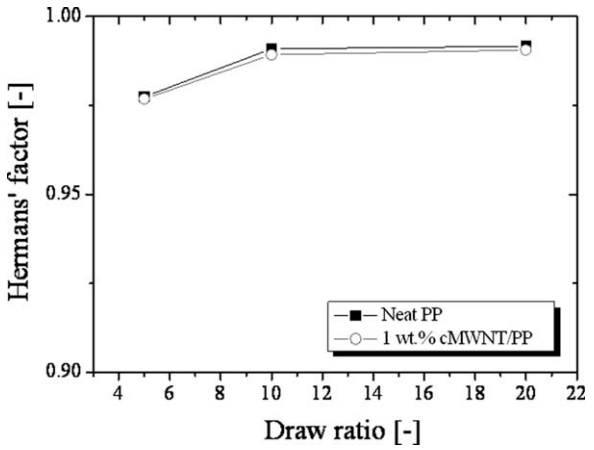

Figure 12 Hermans' orientation factor as a function of draw ratio for neat PP and 1 wt % cMWNT/PP tape.

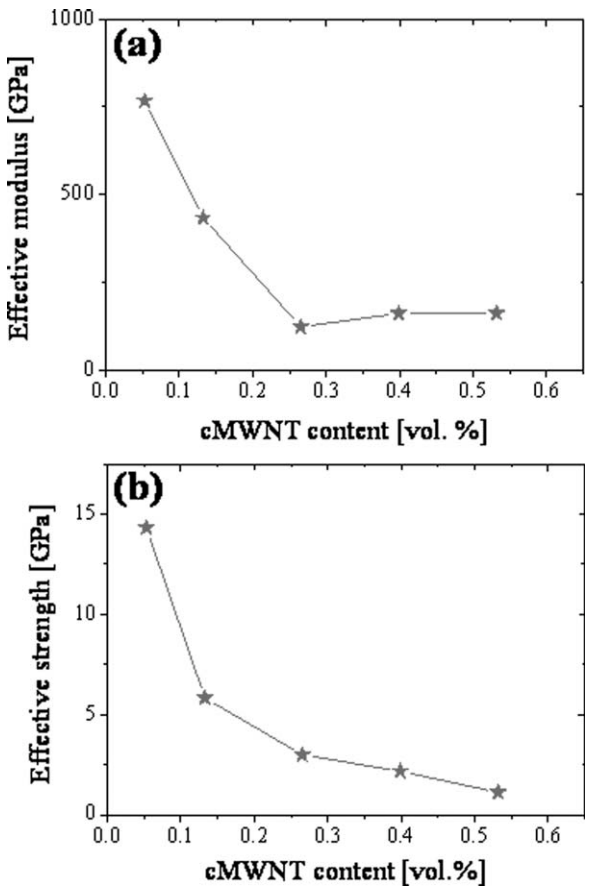

Figure 13 (a) Effective modulus and (b) tensile stress of cMWNTs as calculated from the rule of mixtures for isotropic composites based on PP 3.2 data.

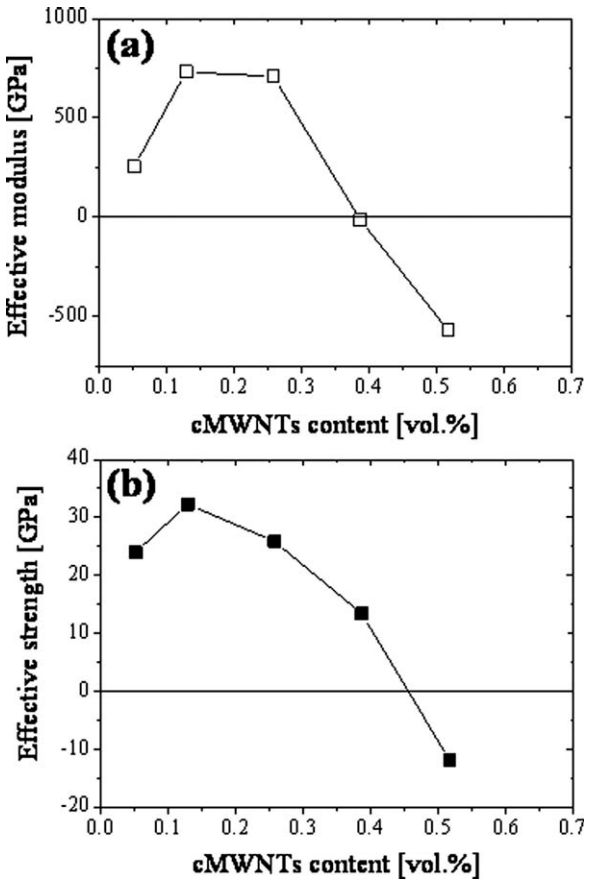

Figure 14 (a) Effective modulus and (b) tensile strength as calculated from the rule of mixtures for oriented (λ = 10) nanocomposite tapes based on PP 3.2 data.

The increase in mechanical properties with the addition of CNTs to PP 1.8 and PP 25 matrix is much higher than the increase observed for PP 3.2 (Figs. 3–4). The reason could be the modification of the matrix through the addition of cMWNTs as indicated by the DSC data shown in Table III. Clearly, cMWNTs have increased the crystallinity of the matrix, and therefore the mechanical property data used for the matrix in eq. (3) and (4) are not the same as those measured for the pure polymer. However, the crystallinity of composites based on PP 3.2 did not change through the addition of cMWNTs. Thus in this case, the effective reinforcement of cMWNTs in the composites based on PP 3.2 can be considered as true contributions of cMWNTs.

Similar calculations can be applied to oriented tapes (λ = 10), but now assuming that both $\eta_0 = 1$ and $\eta_L = 1$, and results are shown in Figure 14. In contrary to isotropic composites, no immediate decrease in reinforcing efficiency of cMWNTs with increasing filler content is observed. By comparing the highest effective properties for both isotropic (λ = 1) and oriented (λ = 10) nanocomposite systems from this study with the values calculated from literature data (see Table VI), it can be seen that the highest effective modulus of CNTs in PP composites is achieved in the current study. The calculated moduli are in the range or approaching values obtained from direct measurement on CNTs,[60–62] however, it is higher than some of the results obtained for CVD-MWNTs.[63] This might be due to the fact that in these studies different MWNTs were used. The effective strength (or stress) of the MWNTs in the oriented tapes in this study is below the data calculated from the paper of Kearns et al.[46] but above all other data. Comparing again with the direct measurement data obtained from AFM test, the calculated strength is indeed approaching the experimental strength data of MWNTs.[64,65] This good result is likely to be caused by the HDPE coating which has improved the dispersion of the MWNTs. The excellent reinforcement of MWNTs in PP matrix at low volume fractions also confirms that the benefit of using high modulus MWNTs in PP fibres or tapes with a relatively low modulus of 15–20 GPa. According to the rule of mixtures, clearly larger quantities of CNTs are needed to obtain a similar relative increase in Young's modulus for high-performance fibres, such as Dyneema®, Kevlar®, Zylon®, or carbon fibres with moduli between 100–400 GPa. Because of the difficulties in dispersing large amounts (>5 wt %) of CNTs effectively in polymer matrices the effective reinforcement of these high-performance fibres by CNTs remains a challenge.[66]

Halpin-Tsai model

Another very popular composite theory is expressed by the Halpin-Tsai equations.[67] The advantage of this model is the possibility of predicting all the elastic constants of composite materials in function of the aspect ratio of the filler, along with the constituent properties and the volume fractions of the two phases. The model will also be employed to compare the theoretical reinforcement of MWNTs in isotropic and oriented PP composites.

TABLE VI
Calculated Effective Mechanical Properties (Using Eq 3 and 4) of MWNTs in Both Isotropic and Oriented Polymer Composites Compared with Data Reported in Literature

Type of CNT	Matrix	E_f [GPa]	σ_f [GPa]	Reference
MWNT	PP	767	14.3	This study, λ = 1
MWNT	PP	732	32	This study, λ = 10
SWNT	PP	610	56	Kearns and Shambaugh[46]
MWNT	PP	497	5.5	Dondero and Gorga[48]
MWNT	PP	305	15.3	Jose et al.[49]
SWNT	PP	100	1.5	Chang et al.[16]
CNF	PP	~ 10	–	Hine et al.[56]

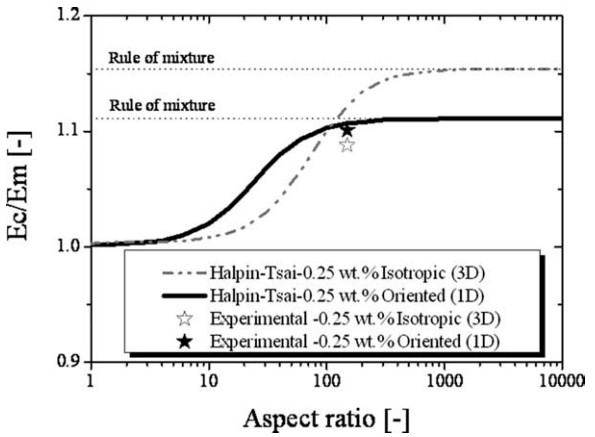

Figure 15 Reinforcement of 0.25 wt % of cMWNTs in uniaxially oriented and 3D isotropic PP composites. The lines are calculated according to Halpin-Tsai theory, and the plateau indicated by the dash line is calculated by rule of mixture.

The Halpin-Tsai equation can be written as

$$\frac{E_c}{E_m} = \frac{1 + \zeta\eta\varphi_f}{1 - \eta\varphi_f} \tag{5}$$

where:

$$\eta = \frac{\left(\frac{E_f}{E_m} - 1\right)}{\left(\frac{E_f}{E_m} + \zeta\right)} \tag{6}$$

In this formula the following parameters can be identified:

E_c = composite modulus
E_m = matrix modulus
E_f = filler modulus
φ_f = volume fraction of the filler
ζ = shape factor

It should be stressed that the Halpin-Tsai set of equations was initially developed for fibre reinforced composites. The modulus for 1D unidirectional and 3D isotropic composites and parameter ζ are given in literature [68,69]:

For 1D unidirectional composites: $E = E_{11}$, $\zeta = (0.5s)^{1.8}$

For 3D isotropic composites:

$$E_{3D-random-Fibre} \approx 0.184 \cdot (E_{\parallel}) + 0.816 \cdot (E_{\perp})$$

$E_{\parallel}$ and $E_{\perp}$ are the elastic moduli of the composite in the longitudinal direction (E_{11}) and in the transverse direction (E_{22}), respectively; and they coincide with the highest and lowest value, for E_{22}, $\zeta = 2$.[68]

The parameter s is the aspect ratio of the filler.[69] It is generally defined as the ratio of the longest and shorter dimension of the filler, i.e. the ratio of the length over the diameter for CNTs. Assuming that the elastic modulus of MWNT is about 700 GPa,[60–62] the elastic modulus of isotropic PP is 1.25 GPa and 9.2 GPa for oriented PP, the filler volume fraction is fixed at 0.129 vol % (0.25 wt %), and the aspect ratio of the coated MWNTs is 150, [70] then the plots shown in Figure 15 can be generated.

Figure 15 shows that the experimental data of isotropic and oriented ($\lambda = 10$) composites fits well with the calculation according to Halpin-Tsai, which confirms that the HDPE coating on MWNT has indeed improved their dispersion as well as created an effective interphase as discussed above. It also shows that the fibre aspect ratio needed to achieve optimum mechanical properties is much lower for oriented composites (>200) than for isotropic composites (>1000), indicating indicate that, to achieve good reinforcement efficiency, oriented fibres are preferred.

CONCLUSIONS

MWNTs were melt compounded with PP matrix and the effect of melt viscosity of the matrix and a HDPE coating on MWNTs was investigated. Morphological studies showed that the polymer with the lowest melt index leads to the best dispersion under similar processing conditions. In terms of the HDPE coated MWNTs, TEM and DSC studies confirmed the existence of HDPE at the interphase between PP and MWNTs in the composites, even after compounding.

The mechanical properties of isotropic composites based on different PP matrices were studied. According to the rule of mixture, a good reinforcing efficiency of MWNTs was only obtained at relatively low filler contents (<0.5 wt %) since dispersion becomes worse at higher loadings. DMA results showed a similar increase in storage modulus, but also indicated a decrease in T_g with increasing filler content.

In the case of oriented nanocomposite tapes, highly oriented MWNTs are observed by SEM while highly oriented polymer crystals are characterized by WAXD. Better mechanical reinforcement of MWNTs is achieved at relatively low draw ratios ($\lambda = 10$). Again, rule of mixture calculations showed that the reinforcing efficiency of CNTs decreased with increasing filler content. The highest effective mechanical properties of coated MWNTs in oriented PP tapes (Young's modulus = 732 GPa and tensile stress = 32 GPa) achieved in this study are very high compared with other composite data reported in literature, and approach theoretical values for MWNTs. Micromechanical calculations based on Halpin-Tsai equations confirms that good stress transfer and dispersion was achieved by using HDPE coated MWNTs and relatively low loadings.

References

1. Coleman, J. N.; Khan, U.; Blau, W. J.; Gun'ko, Y. K. Carbon 2006, 44, 1624.
2. Coleman, J. N.; Khan, U.; Gun'ko, Y. K. Adv Mater 2006, 18, 689.
3. Dubois, P.; Alexandre, M. Adv Eng Mater 2006, 8, 147.
4. Moniruzzaman, M.; Winey, K. Macromolecules 2006, 39, 5194.
5. Thostenson, T. E.; Ren, Z.; Chou, W. T. Compos Sci Technol 2001, 61, 1899.
6. Breuer, O.; Sundararaj, U. Polym Compos 2004, 25, 63.
7. Ciselli, P.; Wang, Z.; Peijs, T. Mater Technol 2007, 22, 10.
8. Deng, H.; Skipa, T.; Zhang, R.; Lellinger, D.; Bilotti, E.; Alig, I.; Peijs, T. Polymer 2009, 50, 3747.
9. Deng, H.; Zhang, R.; Bilotti, E.; Peijs, T.; Loos, J. J Appl Polym Sci 2009, 113, 742.
10. Zhang, R.; Dowden, A.; Deng, H.; Baxendale, M.; Peijs, T. Compos Sci Technol 2009, 69, 1499.
11. Ajayan, P. M.; Stephan, O.; Colliex, C.; Trauth, D. Science 1994, 265, 1212.
12. Wang, Z.; Ciselli, P.; Peijs, T. Nanotechnology 2007, 18, 455709.
13. Andrews, R.; Jacques, D.; Minot, M.; Rantell, T. Macromol Mater Eng 2002, 287, 395.
14. Assouline, E.; Lustiger, A.; Barber, A. H.; Cooper, A. C.; Klein, E.; Wachtel, E.; Wagner, D. H. J Polym Sci Part B: Polym Phys 2003, 41, 520.
15. Bhattacharyya, A. R.; Sreekumar, T. V.; Liu, T.; Kumar, S.; Ericson, L. M.; Hauge, H.; Smalley, R. E. Polymer 2003, 44, 2373.
16. Chang, T. E.; Jensen, L. R.; Kisliuk, A.; Pipes, R. B.; Pyrzand, R.; Sokolov, A. P. Polymer 2005, 46, 439.
17. Grady, B. P.; Bompeo, F.; Shambaugh, R. L.; Resasco, D. E. J Phys Chem B 2002, 106, 5852.
18. Leelapornpisit, W.; Ton-That, M.; Perrin-Sarazin, F.; Cole, K. C.; Denault, J.; Simard, B. J Polym Sci Part B: Polym Phys 2005, 43, 2445.
19. Manchado, M. L. A.; Valentini, L.; Biagiottiand, J.; Kenny, J. M. Carbon 43, 2005, 1499.
20. Seo, M.; Lee, J.; Park, S. Mater Sci Eng A 2005, 404, 79.
21. Seo, M.; Park, S. Chem Phys Lett 2004, 395, 44.
22. Valentini, L.; Biagiotti, J.; Kenny, J. M.; Santucci, S. Compos Sci Technol 2003, 63, 1149.
23. Valentini, L.; Biagiotti, J.; Manchado, M. A. L.; Santucci, S.; Kenny, J. M. Polym Eng Sci 2004, 44, 303.
24. Ganb, M.; Satapathy, B. K.; Thunga, M.; Weidisch, R.; Potschke, P.; Jehnichen, D. Acta Mater 2008, 56, 2247.
25. Peijs, T.; Jacobs, M. J. N.; Lemstra, P. J. In: Comprehensive Composites; Chou, T. W., Kelly, A., Zweben, C., Eds.; Elsevier Science Publishers Ltd: Oxford, 2000; pp 263–302.
26. Ward, I. M. Plast Rubbers Compos 2004, 33, 189.
27. Smith, P.; Lemstra, P. J. J Mater Sci 1980, 15, 505.
28. Kwolek, S. L.; Morgan, P. W.; Schaefgen, J. R.; Gulrich, L. W. Macromolecules 1977, 10, 1390.
29. Ward, I. M.; Hine, P. J. Polymer, 2004, 45, 1413.
30. Alcock, B.; Cabrera, N. O.; Barkoula, N. M.; Loos, J.; Peijs, T. Compos A 2006, 37, 716.
31. Alcock, B.; Cabrera, N. O.; Barkoula, N. M.; Loos, J.; Peijs, T. J Appl Polym Sci 2007, 104, 118.
32. Alcock, B.; Cabrera, N. O.; Barkoula, N. M.; Peijs, T. Compos Sci Technol 2006, 66, 1724.
33. Alcock, B.; Cabrera, N. O.; Barkoula, N. M.; Reynolds, C. T.; Govaert, L. E.; Peijs, T. Compos Sci Technol 2007, 67, 2061.
34. Alcock, B.; Cabrera, N. O.; Barkoula, N. M.; Spoelstra, A. B.; Loos, J.; Peijs, T. Compos A 2007, 38, 147.
35. Alcock, B.; Cabrera, N. O.; Barkoula, N. M.; Wang, Z.; Peijs, T. Compos B 2008, 39, 537.
36. Alcock, B.; Cabrera, N. O.; Barkoula, N.-M.; Loos, J.; Peijs, T. J Appl Polym Sci 2007, 104, 118.
37. Alcock, B.; Cabrera, N. O.; Barkoula, N.-M.; Peijs, T. Compos Sci Technol 2006, 66, 1724.
38. Alcock, B.; Cabrera, N. O.; Barkoula, N.-M.; Spoelstra, A. B.; Loos, J.; Peijs, T. Compos A 2006, 37, 716.
39. Alcock, B.; Cabrera, N. O.; Barkoula, N.-M.; Spoelstra, A. B.; Loos, J.; Peijs, T. Compos A 2007, 38, 147.
40. Barkoula, N. M.; Alcock, B.; Cabrera, N. O.; Peijs, T. Polym Polym Compos 2008, 16, 101.
41. Barkoula, N.-M.; Schimanski, T.; Loos, J.; Peijs, T. Polym Compos 2005, 261, 114.
42. Cabrera, N. O.; Alcock, B.; Klompen, E. T. J.; Peijs, T. Appl Compos Mater 2008, 15, 27.
43. Cabrera, N. O.; Alcock, B.; Peijs, T. Compos B 2008, 39, 1183.
44. Loos, J.; Schimanski, T.; Hofman, J.; Peijs, T.; Lemstra, P. J. Polymer 2001, 42, 3827.
45. www.pure-composites.com.
46. Kearns, J. C.; Shambaugh, R. L. J Appl Polym Sci 2002, 86, 2079.
47. Moore, E. M.; Ortiz, D. L.; Marla, V. T.; Shambaugh, R. L.; Grady, B. P. J Appl Polym Sci 2004, 93, 2926.
48. Dondero, W. E.; Gorga, R. E. J Polym Sci Part B: Polym Phys 2005, 44, 864.
49. Jose, M. V.; Dean, D.; Tyner, J.; Price, G.; Nyairo, E. J Appl Polym Sci 2007, 103, 3844.
50. Fornes, T. D.; Yoon, P. J.; Keskkula, H.; Paul, D. R. Polymer 2001, 42, 9929.
51. Huang, Y. Y.; Ahir, S. V.; Terentjev, E. M. Phys Rev B 2006, 73, 12542.
52. McCurm, N. G.; Buckley, C. P.; Bucknall, C. B. Principles of Polymer Engineering, Oxford University Press Inc.: New York, 1997.
53. Van der Vegt, A. K. From Polymers to Plastics, VSSD: Delft, 2006.
54. Miltner, H. E.; Grossiord, N.; Lu, K. B.; Loos, J.; Koning, C. E.; Van Mele, B. Macromolecules, 2008, 41, 5753.
55. Loos, J.; Schimanski, T. Macromolecules, 2005, 38, 10678.
56. Hine, P.; Broome, V.; Ward, I. Polymer, 2005, 46, 10936.
57. Vaisman, L.; Larin, B.; Davidi, I.; Wachtel, E.; Marom, G.; Wagner, H. D. Compos A 2007, 38, 1354.
58. Van der Heijden, P. C.; Rubatat, L.; Diat, O. Macromolecules, 2004, 37, 5327.
59. Cox, H. L. Brazil J Appl Phys 1952, 3, 72.
60. Xie, S. S.; Li, W. Z.; Pan, Z. W.; Chang, B. H.; Sun, L. F. J Phys Chem Solids 2000, 61, 1153.
61. Treacy, M. M. J.; Ebbesen, T. W.; Gibson, J. M. Nature 1996, 381, 678.
62. Wong, E. W.; Sheehan, P. E.; Lieber, C. M. Science 1997, 277, 1971.
63. Salvetat, J. P.; Kulik, A. J.; Bonard, J. M.; Briggs, G. A. D.; Stockli, T.; Metenier, K.; Bonnamy, S.; Beguin, F.; Burnham, N. A.; Forro, L. Adv Mater 1999, 11, 161.
64. Barber, A. H.; Kaplan-Ashiri, I.; Cohen, R. E.; Tenne, R.; Wagner, H. D. Compos Sci Technol 2005, 65, 2380.
65. Yu, M. F.; Lourie, O.; Dyer, M. J.; Kelly, T. F.; Ruoff, R. S. Science 2000, 287, 637.
66. Ciselli, P.; Zhang, R.; Wang, Z.; Reynolds, C. T.; Baxendale, M.; Peijs, T. Eur Polym J 2009, 45, 2741.
67. Halpin, J. C.; Kardos, J. L. Polym Eng Sci 1976, 16, 344.
68. Van Es, M. Ph. D. Thesis, TU Delft, Delft, 2001.
69. Hull, D.; Clyne, T. W. An Introduction to Composite Materials, 2nd ed.; Cambridge University Press: Cambridge, 1996.
70. Nanocyl S. A. Belgium, 2007.